

# Mechanism of epitaxial self-assembly of Fe nanowedge islands on Mo(110)

I. V. Shvets<sup>1</sup>, S. Murphy, N. Berdunov, V. Usov, G. Mariotto

*SFI Nanoscience Laboratory, Physics Department, Trinity College, Dublin 2,  
Ireland*

S. Makarov

*Allegro Technologies Ltd., Unit 8, Enterprise Centre, Pearse St., Dublin 2, Ireland*

---

## Abstract

The deposition of Fe films in a nominal thickness range of  $2.5 \leq d \leq 8$  Å on the Mo(110) surface at elevated temperatures results in the formation of distinctive nanowedge islands supported on a pseudomorphic Fe layer. We propose a model explaining the growth mode of these wedge-shaped Fe islands. The model is based on the strain produced in the substrate around each island, by the lattice mismatch between the film and substrate. Fe adatoms migrate towards the islands due to the influence of this strain, which is related to the thickness and size of each island. The adatoms subsequently enter the islands not only through their thin ends where the island can be only two monolayers thick but on the contrary, through a vertical climb along the sides of the thicker end, which can be tens of layers thick. This mode

of mass transport is again driven by strain, corresponding to the energy reduction through movement towards the location where the interatomic spacing in the island corresponds to the bulk value. A key element of the model is that misfit dislocations are formed in the lower layers of the nanowedge, which act as migration channels for the vertical climb.

*Key words:* self-assembly, strain, scanning tunneling microscopy, iron, molybdenum

*PACS:* 68.55.-k, 68.55.-a, 81.15.Aa, 81.16.Dn, 68.37.Ef

---

## 1 Introduction

The concept of nanopatterning of surfaces through self-assembly of heteroepitaxially grown nanostructures has received significant attention in recent years with regard to meeting the increasing demands for miniaturization in high-tech applications. Examples are to be found in metal [1], semiconductor [2,3] and insulator [4,5,6] heteroepitaxy, where a variety of nanostructures such as nanowires, pyramids or hut-shaped islands can be formed. In many cases, the self-assembly process is underpinned by the strain relaxation behaviour within the system. We consider the case for the Fe/Mo(110) epitaxial system, where there is a large lattice mismatch of  $(a_{Fe} - a_{Mo})/a_{Mo} = -8.9\%$ . In earlier studies of epitaxial Fe growth on Mo(110) [7,8], it was demonstrated that under certain conditions the deposited films are characterised by the formation of ar-

---

<sup>1</sup> Corresponding author: Fax: (+)353 1 6083228, E-mail: ivchvets@tcd.ie

rays of nanoscale wedge-shaped islands that range in thickness from one or two atomic layers at their thin end to many layers thickness at the other (Fig. 1). These nanowedges always grow in such a way as to maintain a continuous (110) surface that is unbroken by steps. Similar nanowedge islands have been obtained by depositing Fe, Cu, Ni and Ho on W(110) substrates [9,10,11,12] and Pb on Si(111) [13]. It is likely that under the correct growth conditions this growth mode can also be obtained in other epitaxial systems. So far, no significant attempt has been made to understand the reason for this growth mode. In this study, we explore the mechanisms guiding the nanowedge formation in the Fe/Mo(110) epitaxial system and show how they are linked to the mismatch-induced strain.

## 2 Experimental

The experimental results were obtained on two different Mo(110) surfaces. The first had a miscut of  $0.65^\circ$  from the (110) plane, corresponding to an average terrace width of  $\sim 200$  Å with monatomic steps aligned parallel to the  $[1\bar{1}\bar{1}]$  direction. The second was a vicinal surface with a  $4.6^\circ$  miscut from the (110) plane, corresponding to an average terrace width of  $\sim 25$  Å with monatomic steps oriented perpendicular to the  $[1\bar{1}\bar{1}]$  crystallographic direction. The film deposition and analysis were performed in a multi-chamber ultra-high vacuum (UHV) system with a base pressure in the low  $10^{-10}$  torr.

The substrate was cleaned by annealing in  $5 \times 10^{-7}$  torr  $O_2$  at temperatures in the  $1300 \leq T \leq 1500$  K range for 30-60 min cycles, followed by flash-annealing several times to 2400 K for 10-15 s intervals in UHV. The Fe films were deposited by electron beam evaporation of a 3N purity Fe rod. The chamber pressure typically remained below  $2 \times 10^{-10}$  torr during deposition. A quartz crystal balance was used to monitor the deposition rate, which typically lay between 0.006 and  $0.03 \text{ \AA s}^{-1}$ . The deposition stage was equipped with a resistive heater and a k-type thermocouple to allow deposition on substrates at elevated temperatures. The STM results were obtained in constant current mode using a home-built instrument with either W or MnNi tips [14].

### 3 Results and discussion

The mechanisms guiding the formation of these nanowedge structures can be separated into three distinct terms: (1) the initial stages of nanowedge formation from nanowires produced in the first and second Fe layers, (2) the subsequent migration of adatoms towards the nanowedges and (3) the adatom migration within the thickening wedge.

#### *3.1 Initial stages of nanowedge formation*

The first Fe layer and up to  $\sim 80$  % of the second layer form nanowires on Mo(110) by the step-flow growth mechanism in the  $495 \leq T \leq 525$  K temper-

ature range. The intermixing of Fe with the Mo(110) surface can be neglected for substrate temperatures up to 800 K [15]. Despite the large lattice mismatch, the first Fe layer grows pseudomorphically on Mo(110) due to the difference in surface energies between molybdenum ( $\gamma_{Mo} = 2.95 \text{ J.m}^{-2}$ ) and iron ( $\gamma_{Fe} = 2.55 \text{ J.m}^{-2}$ ) [16], which compensates for the large tensile strain accommodated by this layer. However, the increase in elastic energy upon addition of a second Fe layer creates favourable conditions for the formation of strain-relieving dislocations. Dislocation lines are formed along the  $[00\bar{1}]$  direction in second layer nanowires above a critical wire width of the order of 100 Å [8]. The dislocations appear to be randomly distributed in wires that are 130–200 Å wide, but an array of closely-spaced dislocations is found in wires that are 300–600 Å wide [17].

In Fig. 2(a) it is clear that third layer protrusions are formed along some of these dislocation lines. This reflects the preferential nucleation of third layer Fe islands at dislocations in the second Fe layer, which has been observed for Fe films grown on Mo(110) and also on W(110) near room temperature [8,18]. The preferential nucleation is driven by the variation in lattice strain at the dislocation, where the insertion of extra Fe atoms leads to a local compressive strain. The protrusions shown in Fig. 2(a) are the starting point for nanowedge formation. When protrusions on successive terraces overlap and coalesce, small nanowedges are formed, as shown in Fig. 2(b). This is accompanied by a roughening of the step-edges as the second layer nanowires

break up and Fe atoms are absorbed into the developing nanowedge islands.

### *3.2 Adatom migration towards the nanowedge*

Both the presence of surface steps and the two-fold rotational symmetry of Mo(110) give rise to anisotropies in the migration of adatoms on this surface. However, we will show here that the localized strain caused on the surface by the Fe islands governs the migration of adatoms towards the nanowedges.

Although much attention has been paid to the strain in a film caused by a substrate, relatively little attention has been paid to its inevitable consequence - strain in a substrate caused by a film, though the latter can be considerable [19]. To illustrate this point we performed a calculation, using the finite element method, on the simple model of a nanoscale Fe disk bonded to a Mo substrate. The thickness of the disk is 1 nm and its diameter is in the range of 10 to 100 nm. The thickness and the size of the substrate are much greater, so that the substrate could be considered as infinitely large when compared to the disk. The Fe disk is isotropically strained in the radial direction to reflect the lattice mismatch between the disk and the substrate ( $\sim 9\%$ ). The pattern of strain introduced in our model could be formulated as follows: a free non-supported disk is stretched uniformly so that the isotropic strain  $\epsilon_0$  is induced in it and in this expanded state it is bonded to the substrate. The disk attempts to shrink but is held in tensile strain by the substrate. This

introduces a corresponding compressive strain into the substrate beneath the disk.

In the axisymmetric case of an isotropic medium, the strain  $\epsilon$  and stress  $\sigma$  vectors are linked with each other as follows:

$$\sigma = C(\epsilon - \epsilon_0) \quad (1)$$

Here  $\epsilon_0$  stands for the initial strain of the disk to represent the lattice mismatch with the substrate. The strain vector has only four independent components

$$\begin{pmatrix} \epsilon_r \\ \epsilon_\theta \\ \epsilon_z \\ \gamma_{rz} \end{pmatrix} = \begin{pmatrix} \frac{\partial u}{\partial r} \\ \frac{u}{r} \\ \frac{\partial w}{\partial r} \\ \frac{\partial u}{\partial z} + \frac{\partial w}{\partial r} \end{pmatrix} \quad (2)$$

and not six as in the general non-symmetric case.  $r, z, \theta$  are the coordinates of the cylindrical system.  $u$  and  $w$  are the radial and axial displacements respectively and are both independent of  $\theta$ . The tensor

$$C = \frac{E}{(1+\nu)(1-2\nu)} \begin{pmatrix} 1-\nu & \nu & \nu & 0 \\ \nu & 1-\nu & \nu & 0 \\ \nu & \nu & 1-\nu & 0 \\ 0 & 0 & 0 & \frac{1-2\nu}{2} \end{pmatrix} \quad (3)$$

includes the Youngs' modulus  $E$  for the isotropic material and the Poisson's ratio  $\nu$ . We then use the finite element method to find the stress and strain in the disk and the substrate.

Here we use the values for the Youngs' modulae  $E$  of  $211 \times 10^9$  (SI Units) and  $329 \times 10^9$  (SI Units) and Poisson's ratios  $\nu$  of 0.33 and 0.293 for Fe and Mo respectively. One can appreciate that based on the continuum approximation this model has its limitations, in particular when dealing with objects as small as tens of nanometers in size. Besides, one can appreciate that as the films grown are epitaxial, the modulus of elasticity  $E$  has a number of components (in the case of a cubic crystal it contains three components) [20]. However, as this calculation aims at a qualitative rather than quantitative result, we will avoid complications in the model by considering it to be isotropic. Another issue is the elasticity limit; our model assumes that all the deformations remain elastic. In reality, the elasticity limit is exceeded due to the large lattice mismatch between Fe and Mo. Finally, the model does not take into account that the nanowedge islands grow on top of a single pseudomorphic Fe wetting layer, as is the case in the experiment [8].

Figures 3(a) and (b) show the simulated pattern of deformation in a cross-section perpendicular to the surface at the edge of the disk, resulting from the model. In the process of relaxing the tensile strain in the disk, the substrate near the edge of the disk is stretched inwards along the radial direction of relaxation, producing a tensile strain in the substrate around the disk edge. The relaxation also introduces a compressive circumferential strain into the substrate outside the disk edge. Figure 4 shows the dependencies of the radial strain component  $\epsilon_r = \partial u / \partial r$  and circumferential strain component  $\epsilon_\theta = u/r$

at the surface of the substrate as a function of the distance from the centre of the disk. As expected intuitively, the strain falls off more slowly from the disk edge in larger diameter disks, indicating that islands of greater size create larger strained areas in the substrate.

The results of this simple model agree qualitatively with recent atomic scale calculations for Co islands on Cu(111) [21]. These calculations have shown that the Co islands induce an anisotropic strain in the Cu substrate in their vicinity and furthermore, that this strain influences the adatom migration barrier such that adatom motion parallel to an island edge is preferred to adatom motion perpendicular to it. This is due to the fact that for transition metals, the adatom migration barrier generally increases with the surface tensile strain [22], which is reflected by a preference for nucleation on these areas. However, this is not the case for the Fe/Mo(110) system, where we have already observed by STM that Fe adatoms prefer nucleation on top of dislocations where there is a local compressive strain.

The effect of surface strain on the diffusion and nucleation of adatoms must be considered in terms of both the adatom binding energy and the diffusion barrier. In the case of a small tensile strain (1–3 %), the interlayer separation between the first and second layers of the surface is reduced. Consequently, an adatom occupying a hollow site on a surface will experience greater binding to the subsurface atom directly beneath it. This increases the diffusion barrier to an adjacent hollow site. The situation is reversed for a compressively strained

surface, so that the adatom experiences a lowered diffusion barrier. However, in the case of a large tensile strain ( $>3\%$ ), the energy of the bridge site, which the adatom temporarily occupies as it hops between adjacent hollow sites, is also lowered, causing the diffusion barrier to decrease again [23]. This situation can occur in the Fe/Mo(110) system, where the pseudomorphic Fe film must accommodate  $\sim 9\%$  tensile mismatch strain. In this situation, the diffusion barrier across a dislocation may be higher than the diffusion barrier in the tensile regions between the dislocations.

The migration of Fe adatoms towards the nanowedge islands can now be explained in terms of Fig. 5, which illustrates the case of an Fe adatom located on the pseudomorphic Fe wetting layer in the vicinity of an island. A pattern of enhanced tensile strain ( $\geq 9\%$ ) is produced in the surface, which is roughly radial with the center located at the island. Adatom migration along direction 1 leads to a decrease in the adatom diffusion barrier, while direction 2 leads to its increase and directions 3 and 4 are energetically equivalent. The net result is an anisotropic migration of adatoms along the direction of radial strain towards the Fe islands. As the size of the strained area is dependent on the size of the island, the separation between the islands increases with their size, which is typically what is observed by STM. It is also expected that the adatom migration will be directed towards the thicker end of each nanowedge, which produces a greater strain in the surface.

### 3.3 Adatom migration within the nanowedge

From the STM evidence shown in Fig. 6(a)-(b), it is clear that depending on the nominal film thickness deposited, the nanowedges can be many Fe layers thick at their *thin* end. Therefore, to explain the later stages of the nanowedge formation, we must adopt a model where the adatoms undertake a vertical climb up each side of the nanowedge. We propose that dislocations in the lower layers of the nanowedges act as migration channels to facilitate this vertical climb model. Dislocation lines and networks are formed in the lower layers of each nanowedge [7,8], which thread to the walls of the island. Climbing up an island wall implies a reduction in the coordination of the adatom as it makes the very first upward step because it loses contact with atoms on the substrate. However, by considering (Fig. 7(a)), our model can explain such vertical transport. If the adatom moves from the position  $\alpha$  to the position  $\beta$ , thereby making the first step up along the vertical wall, it loses contact with the nearest neighbours on the substrate and this increases the energy of the adatom. Following the model of adatom binding energy dependent on the separation between the adatom and its nearest neighbours, we can appreciate that the required reduction in energy of the adatom comes from the fact that the separation between the atoms AB is smaller than the one between the atoms CD, due to the presence of the dislocation. The strongest change in the interatomic separation happens in the immediate vicinity of the dislocation. Therefore, the locations where the dislocation lines exit to the side of the

island become the channels for the vertical climb of adatoms upwards along the island walls.

The introduction of dislocations within the lower layers of the nanowedge produces a sharp reduction in the tensile strain over the first few layers. As a result, the lattice strain within these layers corresponds to the small tensile strain (1–3 %) regime discussed earlier, where the adatom experiences an increased diffusion barrier. The further up the adatom climbs along the vertical wall of the island, the more this tensile strain is reduced, as the interatomic separation approaches the bulk Fe(110) value within the thick end of the nanowedge. This is illustrated in Fig. 6(c), where the surface corrugation of the dislocation network decreases with increasing island thickness because the Fe lattice becomes relaxed. The reduction in tensile strain towards the thick end of the island lends itself to anisotropic surface migration in this direction. This is schematically shown in Fig. 7(b). Adatoms A1, A2, A3 have climbed the wall of the island to the point that is most remote from the substrate where the interatomic separation between the atoms of the wall is closest to the bulk value. Adatom A4 is shown schematically moving up the wall. We could therefore suggest that the walls of the nanowedges can form hanging cliffs with negative slope. Unfortunately, these cannot be readily observed using STM. Likewise, adatoms B1, B2, B3 and B4 deposited on the surface of the island, migrate towards the thick end of the wedge for the same reason. The net effect is that the nanowedge islands continue to develop predominantly

from their thick end.

## 4 Conclusions

We have experimentally observed an interesting film growth mode using the Fe/Mo(110) epitaxial system. The film forms nanowedges, i.e. structures that can be down to one or two monolayers thick at one end and many monolayers thick at the other. The thickness of the nanowedges increases with each atomic terrace step of the substrate so that the top surface of the nanowedge is virtually atomically flat. This growth mode was also observed before in Fe/W(110) system. The growth of nanowedges implies a most peculiar adatom mass transport on the surface, which has not been explained before.

We propose a model explaining the growth of these wedge-shaped islands. The model is based on the strain caused by the lattice mismatch between the film and the substrate. The essential aspect of the model is the strain caused by the nanoscale Fe islands within the substrate. Our model suggests that adatoms migrate towards the islands due to the influence of this strain. The model further suggests that adatoms enter the islands not only through their thin ends where the island is only two monolayers thick but on the contrary, through a vertical climb along the sides, which is driven again by the energy reduction through movement towards the location where the interatomic spacing corresponds to the bulk value.

One of the key elements of the model is that misfit dislocations are formed in the lower layers of the film. This is based on our experimental STM data. The model agrees qualitatively well with our experimental results. However, it is clear that there are aspects of the mass transport that require a more refined model. We expect that self-assembly of these kinds of nanowedges could take place in other systems characterised by large misfit between the film and the substrate. These nanostructures could also have interesting electronic and magnetic properties.

## 5 Acknowledgments

This work was supported by the Science Foundation Ireland under contract 00/PI.1/C042.

## References

- [1] H. Brune, M. Giovannini, K. Bromann, K. Kern, *Nature* 394 (1998) 451.
- [2] K. Brunner, *Rep. Prog. Phys.* 65 (2002) 27.
- [3] C. Teichert, *Phys. Rep.* (2002) 335.
- [4] M. Alexe, J.F. Scott, C. Curran, N.D. Zakharov, D. Hesse, A. Pignolet, *Appl. Phys. Lett.* 73 (1998) 1592.
- [5] M. Batzill, D.E. Beck, B.E. Koel, *Appl. Phys. Lett.* 78 (2001) 2766.

- [6] E. Vasco, R. Dittman, S. Karthäuser, R. Waser, *Appl. Phys. Lett.* 82 (2003) 2497.
- [7] J. Malzbender, M. Pryzbylski, J. Giergiel, J. Kirschner, *Surf. Sci.* 414 (1998) 187.
- [8] S. Murphy, D. Mac Mathúna, G. Mariotto, I.V. Shvets, *Phys. Rev. B* 66 (2002) 195417.
- [9] H. Bethge, D. Heuer, C. Jensen, K. Beshöft, U. Köhler, *Surf. Sci.* 331-333 (1995) 878.
- [10] K. Reshöft, C. Jensen, U. Köhler, *Surf. Sci.* 421 (1999) 320.
- [11] C. Schmidhals, D. Sander, A. Enders, J. Kirschner, *Surf. Sci.* 417 (1998) 361.
- [12] G. Piaszenski, R. Göbel, C. Jensen, U. Köhler, *Surf. Sci.* 454-456 (2000) 712.
- [13] I.B. Altfeder, K.A. Matveev, D.M. Chen, *Phys. Rev. Lett.* 78 (1997) 2815.
- [14] S.F. Ceballos, G. Mariotto, S. Murphy, I.V. Shvets, *Surf. Sci.* 523 (2003) 131.
- [15] M. Tikhov, E. Bauer, *Surf. Sci.* 232 (1990) 73.
- [16] L. Mezey, J. Giber, *Surf. Sci.* 117 (1982) 220.
- [17] S. Murphy, J. Osing, I.V. Shvets, *Surf. Sci.* 547 (2003) 139.
- [18] C. Jensen, K. Reshöft, U. Köhler, *Appl. Phys. A* 62 (1996) 217.
- [19] D. Sander, R. Skomski, C. Schmidhals, A. Enders, J. Kirschner, *Phys. Rev. Lett.* 77 (1996) 2566.

- [20] L.D. Landau, E.M. Lifshitz, Theory of Elasticity, 2nd ed. (Pergammon Press, Oxford, 1970).
- [21] D.V. Tsvilin, V.S. Stepanyuk, W. Hergert, J. Kirschner, Phys. Rev. B 68 (2003) 205411.
- [22] R.F. Sabiryanov, M.I. Larsson, K.J. Cho, W.D. Nix, B.M. Clemens, Phys. Rev. B 67 (2003) 125412.
- [23] H. Brune, K. Bromann, H. Röder, K. Kern, J. Jacobsen, P. Stoltze, K. Jacobsen, J. Nørskov, Phys. Rev. B 52 (1995) R14380.

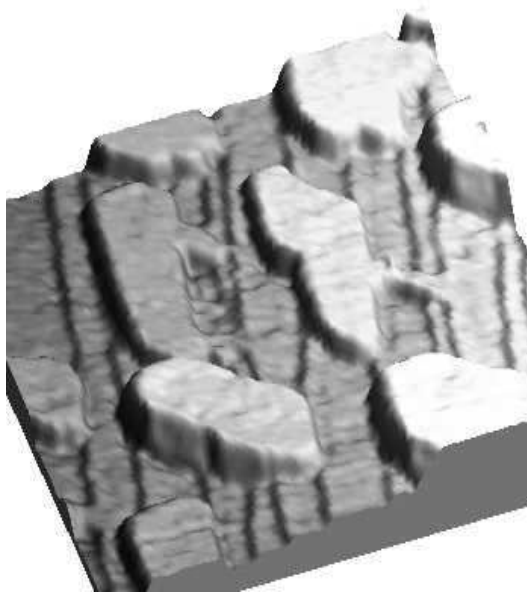


Figure 1. Nanowedge islands typically formed during Fe growth on Mo(110) at elevated temperatures. The nanowedges are formed on top of a closed pseudomorphic Fe layer.

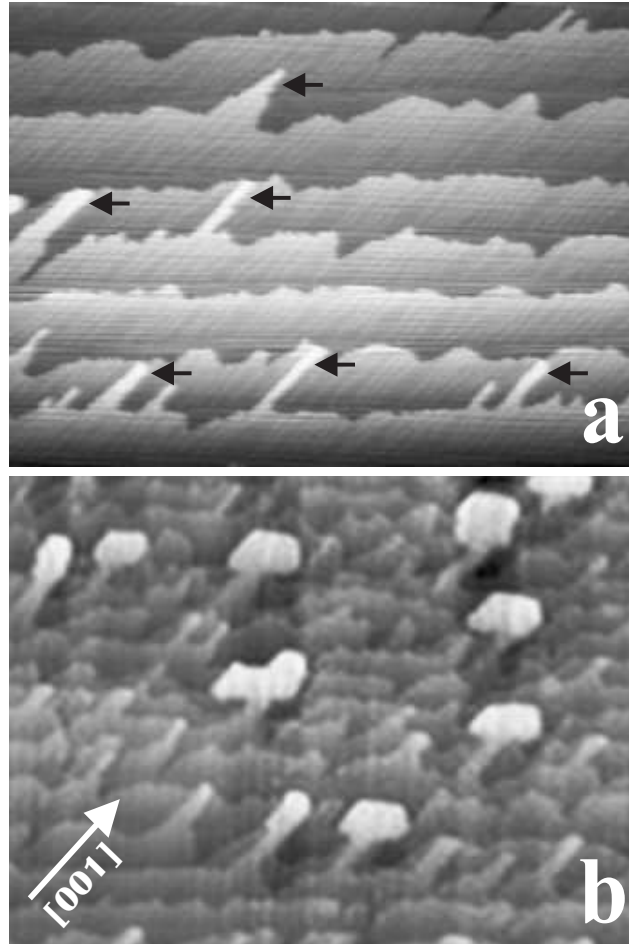


Figure 2.  $500 \text{ nm} \times 350 \text{ nm}$  STM images of a film with  $3 \text{ \AA}$  nominal thickness grown on the low-index  $\text{Mo}(110)$  surface at  $495 \pm 15 \text{ K}$ . (a) Fe third layer protrusions (marked with arrows) are formed on top of some of the dislocation lines in the second Fe layer. (b) Protrusions on successive terraces overlap and coalesce to form small nanowedges.

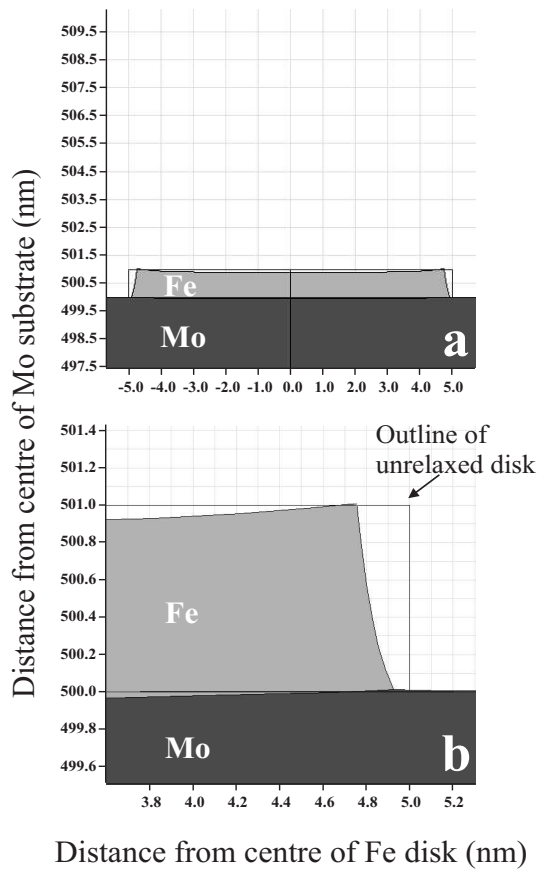


Figure 3. (a) Simulated pattern of deformation in the strained Fe disk and in the Mo substrate. A 10 nm diameter Fe disk (1 nm thick) is strained on top of a Mo substrate, 2000 nm in diameter and 1000 nm thick, and allowed to relax. (b) A zoom-in of the edge of the Fe disk, where the deformation of the disk is evident from the outline of the disk before it is allowed to relax. A local deformation is induced in the substrate near the edge of the disk because the substrate is stretched inwards along the radial direction of relaxation of the disk.

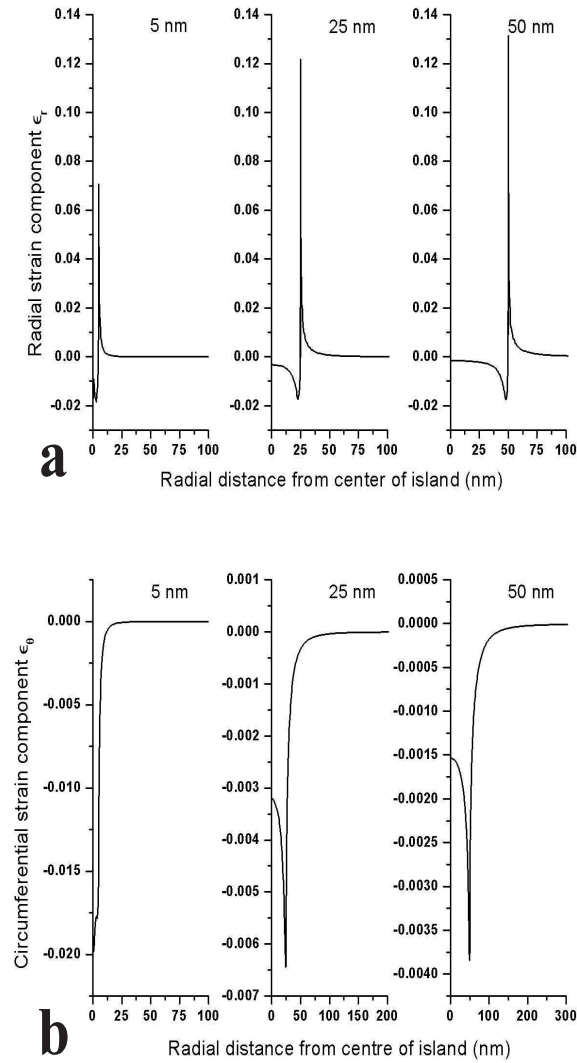


Figure 4. Calculated (a) radial and (b) circumferential strain profiles for a Mo substrate covered by 1 nm thick Fe disks of 5, 25 and 50 nm radii, respectively. (a) The substrate displays a compressive radial strain underneath the Fe disk and a tensile strain in the area outside the disk edge. The radial strain falls off to 1 % of its maximum value at approximately 9, 18 and 22 nm from the edge of the 10, 50 and 100 nm diameter disks, respectively. (b) The circumferential strain in the substrate outside each Fe disk edge is compressive, but is smaller in magnitude than the radial strain.

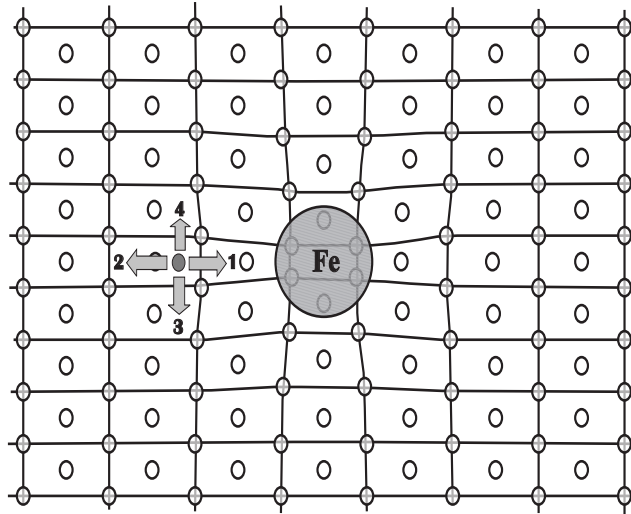


Figure 5. A schematic representation of the tensile strain field produced in the surface around an Fe island. The open circles represent the (110) surface atoms - the surface net is also shown. The large shaded circle is an Fe island, while the dark circle is a single diffusing Fe adatom in a quasi threefold site. The four possible migration directions are indicated.

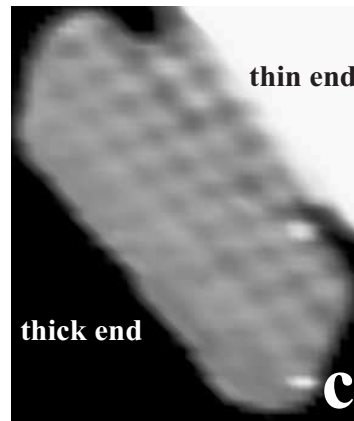
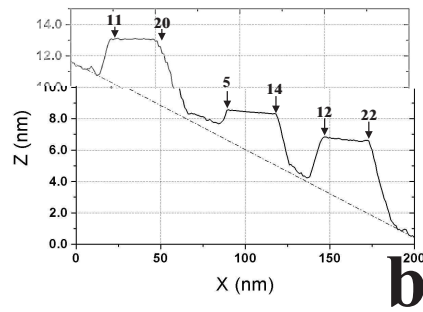
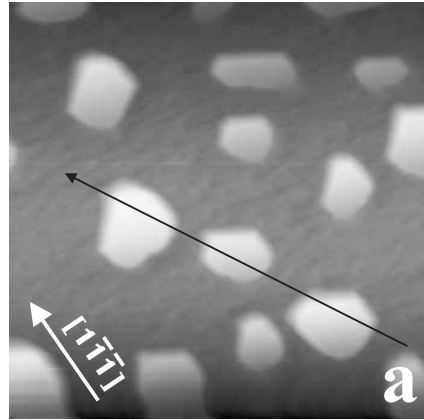


Figure 6. (a) 200 nm × 200 nm STM image of an iron film of 6 Å nominal thickness grown on vicinal Mo(110) at  $700 \pm 25$  K. The black arrow marks the position of the line profile shown in (b), which was taken from the thin end of the nanowedges to their thick end. (b) The local thickness at the thin and thick ends of each nanowedge is indicated by the number of Fe layers. (c) Example of an iron nanowedge where the corrugation produced by the dislocation network decreases towards the thicker end of the island.

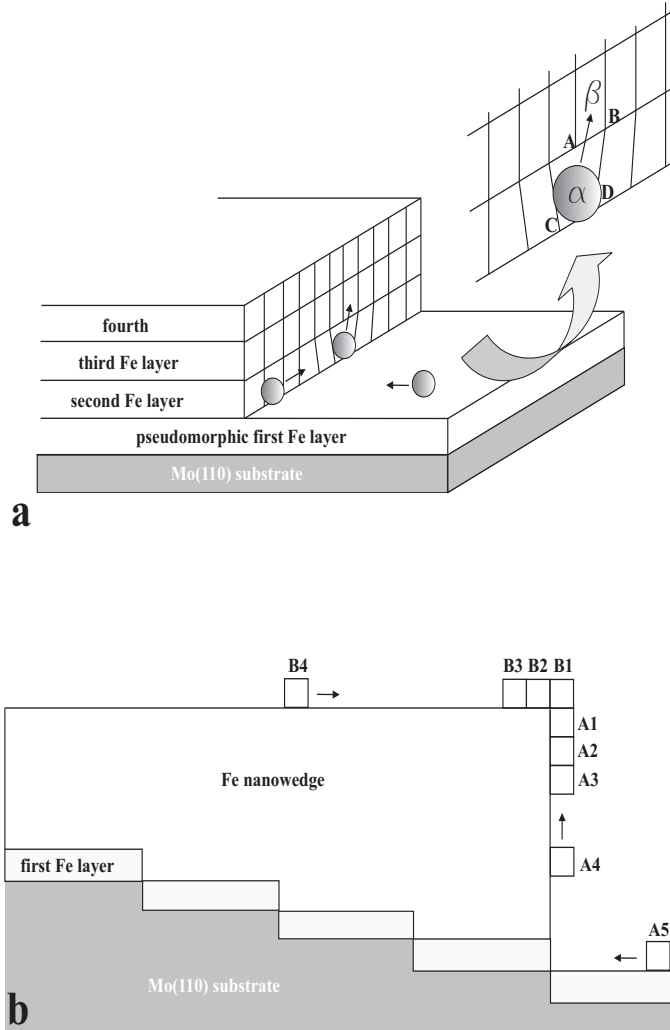


Figure 7. (a) Atoms migrate across the pseudomorphic first Fe layer until they reach the edge of the wedge. They migrate along this edge until they reach the position of a dislocation - this region is enlarged in the insert. Here the interatomic separation  $AB$  in the third Fe layer is smaller than the separation  $CD$  in the second layer. The atom can migrate from position  $\alpha$  to position  $\beta$  despite the energy increase caused by the reduction in coordination, as it is compensated for by the increased adatom binding in position  $\beta$ . (b) Schematic model showing the migration of atoms (A1-A4) up the thick face of a nanowedge to form an overhanging structure. Atoms deposited on the surface of the nanowedge (B1-B4) also migrate towards the thick end of the nanowedge.